AIMS Mathematics, 8(8): 19719–19742.
DOI: 10.3934/math.20231005
Received: 06 April 2023
Revised: 23 May 2023
Accepted: 05 June 2023
Published: 12 June 2023

http://www.aimspress.com/journal/Math

Research article

Dynamical analysis and boundedness for a generalized chaotic Lorenz model

Xinna Mao[1,*], Hongwei Feng[2], Maryam A. Al-Towailb[3] and Hassan Saberi-Nik[4,*]

[1] School of Mathematics and Statistics, Xinxiang University, Xinxiang, Henan 453000, China
[2] School of Civil Engineering and Architecture, Xinxiang University, Xinxiang, Henan 453000, China
[3] Department of Computer Science and Engineering, College of Applied Studies and Community Service, King Saud University, Riyadh, KSA
[4] Department of Mathematics and Statistics, University of Neyshabur, Neyshabur, Iran

* **Correspondence:** Email: maoxinna00319@xxu.edu.cn; saberi_hssn@yahoo.com.

Abstract: The dynamical behavior of a 5-dimensional Lorenz model (5DLM) is investigated. Bifurcation diagrams address the chaotic and periodic behaviors associated with the bifurcation parameter. The Hamilton energy and its dependence on the stability of the dynamical system are presented. The global exponential attractive set (GEAS) is estimated in different 3-dimensional projection planes. A more conservative bound for the system is determined, that can be applied in synchronization and chaos control of dynamical systems. Finally, the finite time synchronization of the 5DLM, indicating the role of the ultimate bound for each variable, is studied. Simulations illustrate the effectiveness of the achieved theoretical results.

Keywords: generalized chaotic Lorenz system; globally exponentially attractive set; ultimate bound set; finite-time synchronization
Mathematics Subject Classification: 34H10, 34H15, 34H20

1. Introduction

Chaos is very interesting nonlinear phenomenon and has applications in many areas such as biology, economics, signal generator design, secure communication, many other engineering systems and so on. Because a nonlinear system in the chaotic state is very sensitive to its initial condition and chaos causes often irregular behavior in practical systems, chaos is sometimes undesirable [1–7]. The 3-dimensional Lorenz model (3DLM) was the first chaotic system proposed in the literature [3]. Celikovsky and Chen [2, 8, 9] introduced generalized Lorenz canonical forms, covering a large class of 3-dimensional

autonomous systems. Further, Zhang et al. [10] by combining the advantages of both integer-order and fractional-order complex chaotic systems, proposed a hybrid-order complex Lorenz system. Chaotic systems have been widely addressed both from their mathematical properties [11, 12] and practical applications [11–15].

The 3DLM reveals the dependence of the solutions on the initial conditions for chaotic situations. Higher order Lorenz models have been derived to further study the stability of solutions and paths to chaos. The 3DLM, was obtained from the Rayleigh-Benard convection equations, which combine dissipative, heating and nonlinear advection physical processes. An interesting topic is the investigation of modes in the 3DLM and its generalization to higher dimensional models by increasing the number of modes. Shen [16, 17] generalized the 3DLM to the 5DLM by adding two additional Fourier modes. This led to a better understanding of the role of some variables in the stability of solutions. Therefore, the 5DLM allows the role of modes in the predictability of solutions to be investigated for further understanding of the variables that increase the stability of solutions, and to find analytical solutions for critical points. Although the role of the modes on the stability of solutions, as well as some dynamical properties of the 5DLM, have been studied, the calculation of bounds for the variables and the global dynamics of the 5DLM are still open and challenging problems. Shen also extended the 5DLM to a six-dimensional Lorenz model (6DLM) [18], seven-dimensional Lorenz model (7DLM) [19] and generalized Lorenz model (GLM) [20], in order to examine the impact of an additional mode and its accompanying heating term on solution stability.

Given a chaotic dynamical system, if its chaotic attractor is bounded in the phase space and the trajectories of the system remain in a bounded region of the phase space, then we say that "the chaotic dynamical system is bounded". Estimation of the ultimate bound set (UBS) and the positive invariant set (PIS) of a chaotic system plays a very important role in studying its dynamic behavior. Among the most important applications, one can mention their use in controlling and synchronizing chaotic systems [21–29]. In fact, the bounds are necessary for both theoretical studies of chaotic attractors and numerical search of attractors. If we can show that, under certain considerations, there exists a GEAS for a chaotic system, then we can conclude that the system cannot have periodic or quasi-periodic responses, equilibrium points, or hidden attractors, outside this set of attractors. This issue has a great application in controlling systems and preventing their possible problems. Leonov [21] derived the first results about global UBS for the Lorenz model. Subsequently, Swinnerton-Dyer [30] demonstrated that the bounds of the states of the Lorenz equations could be determined by using Lyapunov functions. Several researchers further developed the idea and computed the GEAS and PIS for different chaotic systems [31–34].

To the best of our knowledge, the GEAS and UBS for the 5DLM have not been investigated yet. In the present work, by changing system parameters and conditions, we create different attractive sets. Also, we calculate a small attractive set only dependent on the system parameters. The results obtained from the UBS have been used in the synchronization and control of dynamical systems [35–37]. Due to the importance of minimizing the synchronization time, by applying a finite time control scheme, an efficient synchronization method is given based on the obtained ultimate bound [38,39]. By developing these techniques, we can also estimate the ultimate bound of fractional chaotic systems [40–42].

This article is organized into 6 sections. The dynamical behavior of the 5DLM, including phase portraits, bifurcation diagrams and Hamilton energy are given in Section 2. In Section 3, we introduce some preliminary definitions and GEAS of the system. In Section 4, we present a method to compute

small bound for the 5DLM. Section 5 presents the finite time synchronization problem using the results obtained in Section 4. The main conclusions are given in Section 6.

2. Five-dimensional Lorenz model

The Rayleigh-Benard model for 2-dimensional (x, z), dissipative and forced convection is [3]:

$$\frac{\partial}{\partial t}\nabla^2\psi = -\frac{\partial(\psi, \nabla^2\psi)}{\partial(x, z)} + \nu\nabla^4\psi + g\gamma\frac{\partial\theta}{\partial x}, \tag{2.1}$$

$$\frac{\partial}{\partial t}\theta = -\frac{\partial(\psi, \theta)}{\partial(x, z)} + \frac{\Delta T}{H}\frac{\partial\psi}{\partial x} + \kappa\nabla^2\theta. \tag{2.2}$$

According to the studies of Rayleigh [3] and Saltzman [4], the following equations were obtained

$$a(1 + a^2)^{-1}\kappa^{-1}\psi = x_1\sqrt{2}\sin(\pi a H^{-1}x)\sin(\pi H^{-1}z), \tag{2.3}$$

$$\pi R_c^{-1}R_a\Delta T^{-1}\theta = x_2\sqrt{2}\cos(\pi a H^{-1}x)\sin(\pi H^{-1}z) - x_3\sin(2\pi H^{-1}z), \tag{2.4}$$

where, x_1, x_2 and x_3 are function of time alone. All the parameters and variables mentioned above are given in Table 1.

Table 1. The parameters and variables in Eqs (2.1)–(2.5).

Parameter	Meaning
ψ	stream function
θ	temperature perturbation
g	gravity acceleration
γ	thermal expansion coefficient
ν	kinematic viscosity
κ	thermal diffusivity
ΔT	temperature difference
R_a	Rayleigh number
R_c	free-slip critical Rayleigh value
a	ratio of vertical and horizontal scale

By making some changes and manipulations, the partial differential equations (2.1) and (2.2) are converted into ordinary differential equations. Thus, the 3DLM chaotic system is expressed as [3]:

$$\begin{aligned} \dot{x}_1 &= \sigma(x_2 - x_1), \\ \dot{x}_2 &= -x_1x_3 + rx_1 - x_2, \\ \dot{x}_3 &= x_1x_2 - bx_3, \end{aligned} \tag{2.5}$$

where, σ, r are the Prandtl number, normalized Rayleigh number or the heating parameter and $b = \frac{4}{1+a^2}$. Shen et al. [16] extended the 3DLM to the five-dimensional LM (5DLM) by including two additional

Fourier modes with two additional vertical wave numbers. They used the five Fourier modes and rewrote ψ and θ as the following:

$$\psi = \kappa \frac{1+a^2}{a}(x_1 M_1), \tag{2.6}$$

$$\theta = \frac{\Delta T}{\pi}\frac{R_c}{R_a}(x_2 M_2 - x_3 M_3 + x_4 M_5 - x_5 M_6), \tag{2.7}$$

where,

$$\begin{aligned} M_1 &= \sqrt{2}\sin(lx)\sin(mz), \\ M_2 &= \sqrt{2}\cos(lx)\sin(mz), \\ M_3 &= \sin(2mz), \\ M_5 &= \sqrt{2}\cos(lx)\sin(3mz), \\ M_6 &= \sin(4mz). \end{aligned}$$

An additional mode $M_4 = \sqrt{2}\sin(lx)\sin(3mz)$ is included to derive the 6DLM. Here, l and m are defined as $\frac{\pi a}{H}$ and $\frac{\pi}{H}$, representing the horizontal and vertical wave numbers, respectively, and H is the domain height and $\frac{2H}{a}$ represents the domain width.

By coordinate transformation, the original equation can be reduced to the following five-dimensional nonlinear dynamics:

$$\begin{aligned} \dot{x}_1 &= \sigma(x_2 - x_1), \\ \dot{x}_2 &= -x_1 x_3 + r x_1 - x_2, \\ \dot{x}_3 &= x_1 x_2 - x_1 x_4 - b x_3, \\ \dot{x}_4 &= x_1 x_3 - 2x_1 x_5 - d x_4, \\ \dot{x}_5 &= 2x_1 x_4 - 4b x_5, \end{aligned} \tag{2.8}$$

where $d = \frac{9+a^2}{1+a^2}$.

Numerical analysis shows that the dynamical behavior of (2.8) changes from steady-state to chaotic, with the increase of r.

Figure 1 depicts the bifurcation diagram when the parameters values $\sigma = 10, b = \frac{8}{3}$ and $d = \frac{19}{3}$ are fixed, and r varies on the interval $[0, 100]$. In fact, one can see that chaos occurs after $r > 42.5$. For the value of the parameters $\sigma = 10, b = \frac{8}{3}, d = \frac{19}{3}, r = 43$ and $r = 25$, Lyapunov exponents are shown in Figure 2. The values of Lyapunov exponents at 500th second are $L_1 = 1.1281$, $L_2 = 0.0073$, $L_3 = -1.3786$, $L_4 = -1.3774$ and $L_5 = -1.6688$. It is easy to observe that if $r = 43$, then system (2.8) has the positive largest Lyapunov exponent. Therefore, the system (2.8) can exhibit chaotic behaviors. When selecting parameters $\sigma = 10, b = \frac{8}{3}, r = 25$ and $d = \frac{19}{3}$, the values of Lyapunov exponents at 500th second are $L_1 = -0.5246$, $L_2 = -0.5358$, $L_3 = -6.9952$, $L_4 = -2.0305$ and $L_5 = -4.1633$. All negative Lyapunov exponents indicate that the behavior of the system is non-chaotic.

The time responses of the system for $r = 25$ and $r = 43$ are depicted in Figure 3. We verify that the system with $r = 25$ produces a steady-state solution and when $r = 43$ the system is in a chaotic state. Figure 4 depicts the phase portraits of system (2.8) when $\sigma = 10, b = \frac{8}{3}, r = 25$ and $d = \frac{19}{3}$. Figure 5 shows its chaotic behavior with $\sigma = 10, b = \frac{8}{3}, r = 43$ and $d = \frac{19}{3}$.

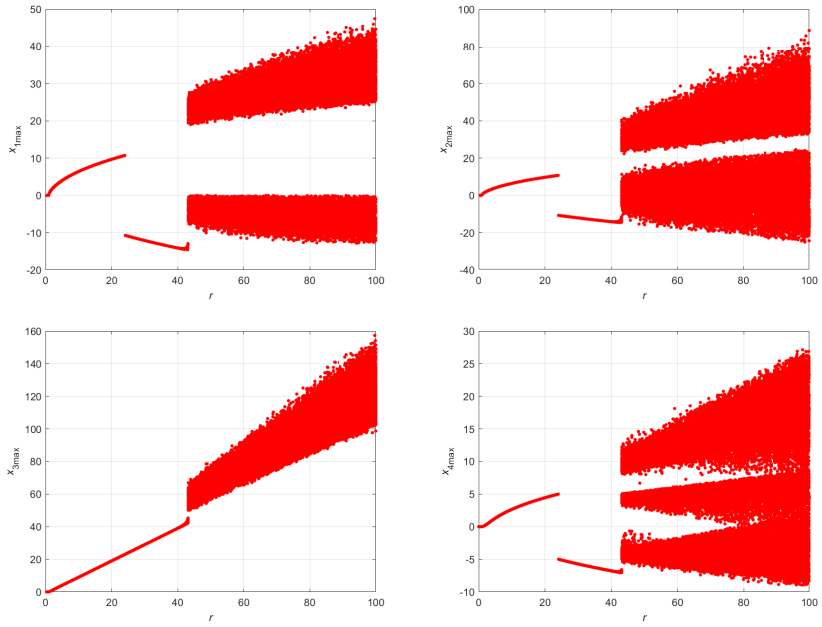

Figure 1. Bifurcation diagram of (2.8) with $\sigma = 10, b = \frac{8}{3}, d = \frac{19}{3}$ and varying r.

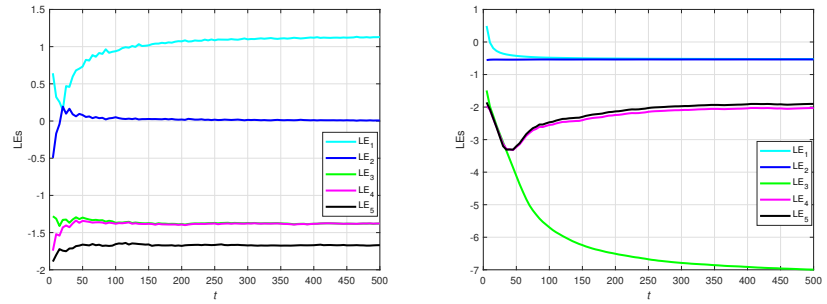

(a) $r = 43$ (b) $r = 25$

Figure 2. Lyapunov exponent spectra for system (2.8) with $\sigma = 10, b = \frac{8}{3}, d = \frac{19}{3}, r = 43$ and $r = 25$.

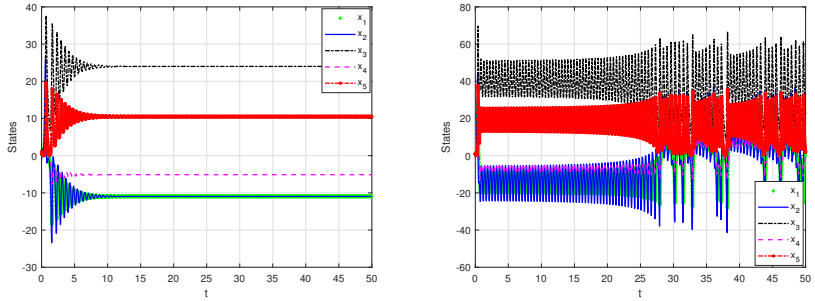

(a) $r = 25$ (b) $r = 43$

Figure 3. State trajectories of (2.8) with $\sigma = 10, b = \frac{8}{3}, d = \frac{19}{3}, r = 25$ and $r = 43$.

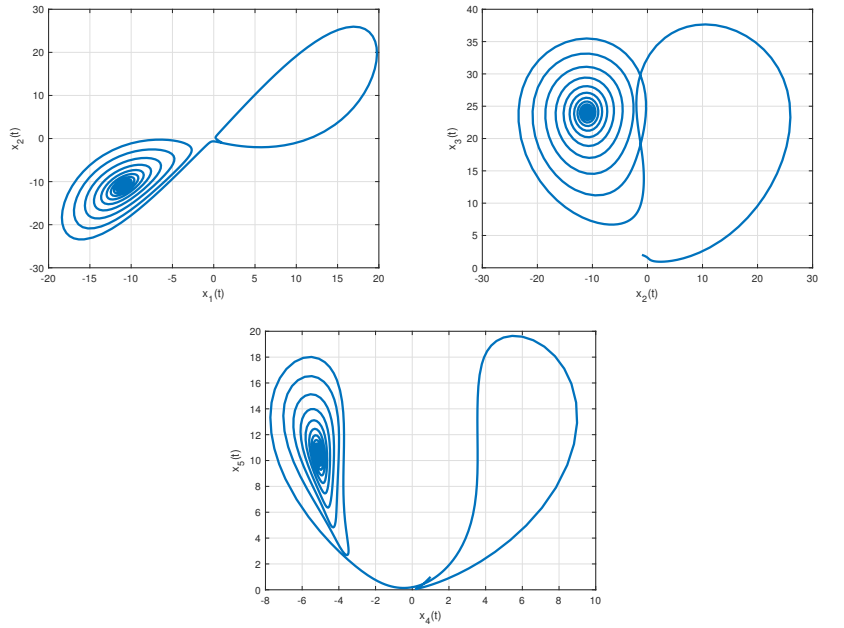

Figure 4. The phase portraits of (2.8) with $\sigma = 10, b = \frac{8}{3}, r = 25$ and $d = \frac{19}{3}$.

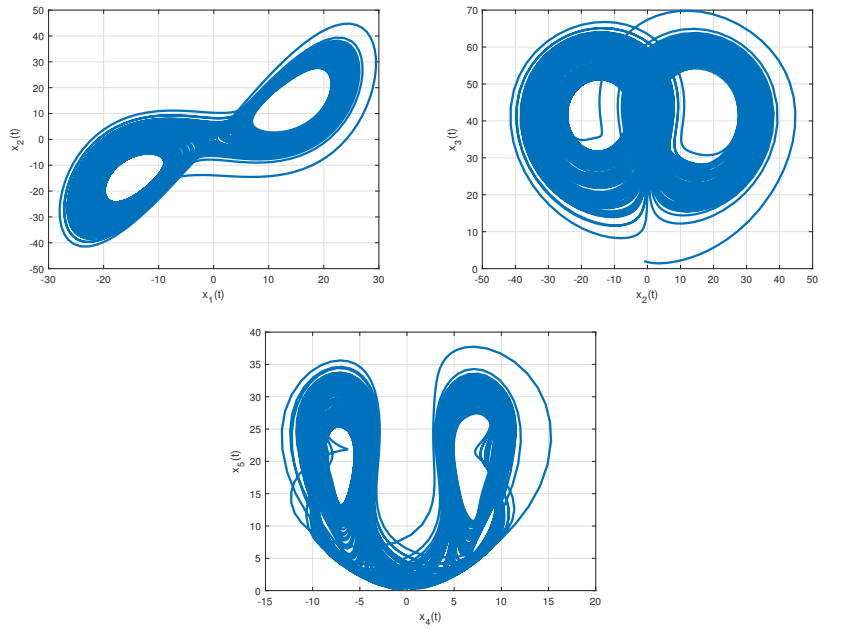

Figure 5. Visualization of the chaotic attractor of (2.8) with $\sigma = 10, b = \frac{8}{3}, r = 43$ and $d = \frac{19}{3}$.

In this section, the Hamilton energy for the 5-dimensional Lorenz model (5DLM) is investigated. The Hamilton energy plays a crucial role in the stability of dynamical systems [43]. By continuously pumping or releasing energy in the system, we are able to stabilize chaos. Furthermore, the relation between the Hamilton energy and different chaotic attractors of system (2.8) and the energy dependence on attractors are discussed. Calculation of Hamilton energy for high-order Lorenz

systems including six-dimensional Lorenz model (6DLM) [18], seven-dimensional Lorenz model (7DLM) [19] and generalized Lorenz model (GLM) [20], can be an interesting topic due to their special physical nature.

Let us rewrite (2.8) in the form:

$$\begin{bmatrix} \dot{x}_1 \\ \dot{x}_2 \\ \dot{x}_3 \\ \dot{x}_4 \\ \dot{x}_5 \end{bmatrix} = F_c + F_d = \begin{bmatrix} \sigma x_2 \\ r x_1 - x_1 x_3 \\ x_1 x_2 - x_1 x_4 \\ x_1 x_3 - 2 x_1 x_5 \\ 2 x_1 x_4 \end{bmatrix} + \begin{bmatrix} -\sigma x_1 \\ -x_2 \\ -b x_3 \\ -d x_4 \\ -4 b x_5 \end{bmatrix}$$

$$= \begin{bmatrix} 0 & \sigma & 0 & 0 & 0 \\ -\sigma & 0 & -x_1 & 0 & 0 \\ 0 & x_1 & 0 & -x_1 & 0 \\ 0 & 0 & x_1 & 0 & -2x_1 \\ 0 & 0 & 0 & 2x_1 & 0 \end{bmatrix} \begin{bmatrix} -\frac{r x_1}{\sigma} \\ x_2 \\ x_3 \\ x_4 \\ x_5 \end{bmatrix} + \begin{bmatrix} \frac{\sigma^2}{r} & 0 & 0 & 0 & 0 \\ 0 & -1 & 0 & 0 & 0 \\ 0 & 0 & -b & 0 & 0 \\ 0 & 0 & 0 & -d & 0 \\ 0 & 0 & 0 & 0 & -4b \end{bmatrix} \begin{bmatrix} -\frac{r x_1}{\sigma} \\ x_2 \\ x_3 \\ x_4 \\ x_5 \end{bmatrix}$$

$$= J(X)\nabla H + R(X)\nabla H,$$

where ∇H stands for the gradient vector of a smooth energy function $H(X)$, $J(X)$ represents a skew-symmetric matrix, and $R(X)$ denotes a symmetric matrix.

The Hamilton energy function can be expressed as:

$$\frac{dH}{dt} = \nabla H^T R(X) \nabla H, \tag{2.9}$$

$$\nabla H^T J(X) \nabla H = 0. \tag{2.10}$$

Using the Helmholtz's theorem [43], it can be represented by:

$$\nabla H^T F_c(X) = 0, \tag{2.11}$$

$$\nabla H^T F_d(X) = \frac{dH}{dt}. \tag{2.12}$$

Thus, we have:

$$H = -\frac{1}{2}\frac{r}{\sigma}x_1^2 + \frac{1}{2}x_2^2 + \frac{1}{2}x_3^2 + \frac{1}{2}x_4^2 + \frac{1}{2}x_5^2. \tag{2.13}$$

Furthermore, it rate of variation is:

$$\frac{dH}{dt} = r x_1^2 - x_2^2 - b x_3^2 - d x_4^2 - 4 b x_5^2. \tag{2.14}$$

Figure 6 illustrates that chaotic and steady-state require lower and higher Hamilton energy, respectively.

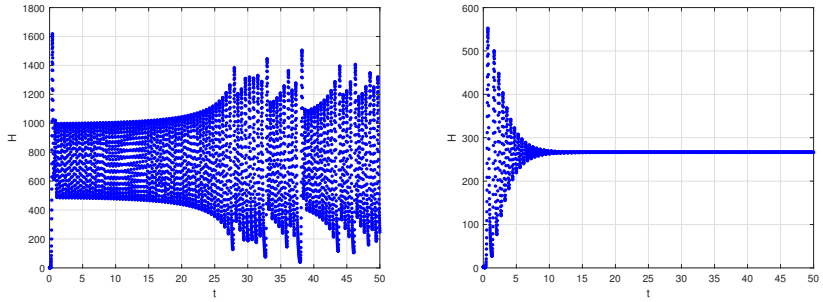

(a) $r = 43$ (b) $r = 25$

Figure 6. The Hamilton energy function H, with $\sigma = 10, b = \frac{8}{3}, d = \frac{19}{3}, r = 25$ and $r = 43$.

3. Ultimate bound sets

In this section, we pursue the goal of proving the existence of GEAS for the chaotic system (2.8). We will first mention a few prerequisites and definitions.

Let $\mathfrak{X} = (x_1, x_2, x_3, x_4, x_5)^T$, and consider that $\mathfrak{X}(t, t_0, \mathfrak{X}_0)$ is the solution of system

$$\frac{d\mathfrak{X}}{dt} = g(\mathfrak{X}), \tag{3.1}$$

that satisfies $\mathfrak{X}_0 = \mathfrak{X}(t_0, t_0, \mathfrak{X}_0)$, with $t_0 \geq 0$ representing the initial time. Also, $g : \mathbb{R}^5 \to \mathbb{R}^5$ and $\Psi \subset \mathbb{R}^5$ is a compact set. Let us define the distance between $\mathfrak{X}(t, t_0, \mathfrak{X}_0)$ and Ψ as:

$$\rho(\mathfrak{X}(t, t_0, \mathfrak{X}_0), \Psi) = \inf_{\mathfrak{Z} \in \Psi} \| \mathfrak{X}(t, t_0, \mathfrak{X}_0) - \mathfrak{Z} \| . \tag{3.2}$$

Denote $\Psi_\gamma = \{\mathfrak{X} \mid \rho(\mathfrak{X}, \Psi) < \gamma\}$. Thus, one gets $\Psi \subset \Psi_\gamma$.

Definition 3.1. *[21]. Suppose that $\Psi \subset \mathbb{R}^5$ is a compact set. If for any $\mathfrak{X}_0 \in \mathbb{R}^5/\Psi$,*

$$\lim_{t \to \infty} \rho(\mathfrak{X}(t), \Psi) = 0,$$

then Ψ is an UBS of (3.1). Moreover, if for any $\mathfrak{X}_0 \in \Psi$ and all $t \geq t_0$, $\mathfrak{X}(t, t_0, \mathfrak{X}_0) \in \Psi$, then Ψ is the PIS for (3.1).

From the above, it is interpreted that having a GEAS for a system guarantees that the system is UBS.

Definition 3.2. *[21]. Given a Lyapunov function $\mathcal{L}_\gamma(\mathfrak{X})$, if there exist constants $K_\gamma > 0$ and $s_\gamma > 0$, such that*

$$\forall \mathfrak{X}_0 \in \mathbb{R}^5,\ \mathcal{L}_\gamma(\mathfrak{X}(t)) - K_\gamma) \leq (\mathcal{L}_\gamma(\mathfrak{X}_0) - K_\gamma)e^{-s_\gamma(t-t_0)}, \tag{3.3}$$

for $\mathcal{L}_\gamma(\mathfrak{X}_0) > K_\gamma$ and $\mathcal{L}_\gamma(\mathfrak{X}) > K_\gamma$, then $\Psi_\gamma = \{\mathfrak{X} | \mathcal{L}_\gamma(\mathfrak{X}(t)) \leq K_\gamma\}$ is a GEAS of (2.8). Moreover, if for any $\mathfrak{X}_0 \in \Psi_\gamma$ and all $t > t_0$, $\mathfrak{X}(t, t_0, \mathfrak{X}_0) \in \Psi_\gamma$, then Ψ_γ is a PIS.

The next theorem introduces the GEAS for system (2.8).

Theorem 3.1. *For any $\sigma > 0$, $b > 0$, $r > 0, d > 0, \beta > 0$ and $\alpha > 0$, with*

$$\mathcal{L}_{\alpha,\beta}(\mathfrak{X}(t)) = \alpha x_1^2 + \beta x_2^2 + \beta x_4^2 + \beta(x_3 - \frac{\sigma\alpha + r\beta}{\beta})^2 + \beta(x_5 - \frac{\sigma\alpha + r\beta}{2\beta})^2, \tag{3.4}$$

$$\epsilon = min\{1, \sigma, b, d\} > 0,$$
$$K_{\alpha,\beta} = \frac{11b}{7\beta\epsilon}(\sigma\alpha + r\beta)^2 > 0,$$
$$\mathfrak{X}(t) = (x_1(t), x_2(t), x_3(t), x_4(t), x_5(t)), \quad \mathfrak{X}(t_0) = (x_1(t_0), x_2(t_0), x_3(t_0), x_4(t_0), x_5(t_0)).$$

If $\mathcal{L}_{\alpha,\beta}(\mathfrak{X}(t)) \geq K_{\alpha,\beta}$, $t \geq t_0$, then

$$\mathcal{L}_{\alpha,\beta}(\mathfrak{X}(t)) - K_{\alpha,\beta} \leq [\mathcal{L}_{\alpha,\beta}(\mathfrak{X}_0) - K_{\alpha,\beta}]e^{-\epsilon(t-t_0)}.$$

This indicates that

$$\Psi_{\alpha,\beta}(\mathfrak{X}(t)) = \left\{\mathfrak{X}|\alpha x_1^2 + \beta x_2^2 + \beta x_4^2 + \beta(x_3 - \frac{\sigma\alpha + r\beta}{\beta})^2 + \beta(x_5 - \frac{\sigma\alpha + r\beta}{2\beta})^2 \leq K_{\alpha,\beta}\right\}$$

is a GEAS and PIS of the system.

Proof. Let us define

$$f(x_5) = -7b\beta x_5^2 + 3b(\sigma\alpha + r\beta)x_5, \tag{3.5}$$

and consider the definite positive Lyapunov function

$$\mathcal{L}_{\alpha,\beta}(\mathfrak{X}(t)) = \alpha x_1^2 + \beta x_2^2 + \beta(x_3 - \frac{\sigma\alpha + r\beta}{\beta})^2 + \beta x_4^2 + \beta(x_5 - \frac{\sigma\alpha + r\beta}{2\beta})^2. \tag{3.6}$$

The derivative of $\mathcal{L}_{\alpha,\beta}$ is as follows

$$\begin{aligned}
\frac{d\mathcal{L}_{\alpha,\beta}}{dt} &= 2\alpha x_1\dot{x}_1 + 2\beta x_2\dot{x}_2 + 2\beta(x_3 - \frac{\sigma\alpha + r\beta}{\beta})\dot{x}_3 + 2\beta x_4\dot{x}_4 + 2\beta(x_5 - \frac{\sigma\alpha + r\beta}{2\beta})\dot{x}_5 \\
&= 2\alpha x_1(\sigma x_2 - \sigma x_1) + 2\beta x_2(-x_1x_3 + rx_1 - x_2) \\
&\quad + 2\beta(x_3 - \frac{\sigma\alpha + r\beta}{\beta})(x_1x_2 - x_1x_4 - bx_3) \\
&\quad + 2\beta x_4(x_1x_3 - 2x_1x_5 - dx_4) + 2\beta(x_5 - \frac{\sigma\alpha + r\beta}{2\beta})(2x_1x_4 - 4bx_5) \\
&= -\sigma\alpha x_1^2 - \beta x_2^2 - \beta b(x_3 - \frac{\sigma\alpha + r\beta}{\beta})^2 - \beta d x_4^2 - b\beta(x_5 - \frac{\sigma\alpha + r\beta}{2\beta})^2 - \sigma\alpha x_1^2 \\
&\quad - \beta x_2^2 - b\beta x_3^2 - \beta d x_4^2 - 7b\beta x_5^2 + \frac{5b}{4\beta}(\sigma\alpha + r\beta)^2 + 3b(\sigma\alpha + r\beta)x_5.
\end{aligned}$$

From (3.5) we have

$$\max_{x\in\mathbb{R}} f(x_5) = \frac{9b}{28\beta}(\sigma\alpha + r\beta)^2, \tag{3.7}$$

therefore,

$$\frac{d\mathcal{L}_{\alpha,\beta}}{dt} \leq -\sigma\alpha x_1^2 - \beta x_2^2 - \beta b(x_3 - \frac{\sigma\alpha + r\beta}{\beta})^2 - \beta d x_4^2 - b\beta(x_5 - \frac{\sigma\alpha + r\beta}{2\beta})^2 + \frac{11b}{7\beta}(\sigma\alpha + r\beta)^2 \leq -\epsilon\mathcal{L}_{\alpha,\beta}(\mathfrak{X}(t)) + \epsilon K_{\alpha,\beta} < 0, \tag{3.8}$$

when $\mathcal{L}_{\alpha,\beta}(\mathfrak{X}(t)) \geq K_{\alpha,\beta}$. Then, we have the equivalent

$$\begin{aligned}\mathcal{L}_{\alpha,\beta}(\mathfrak{X}(t)) &\leq \mathcal{L}_{\alpha,\beta}(\mathfrak{X}(t_0))e^{-\epsilon(t-t_0)} + \int_{t_0}^{t} \epsilon e^{-\epsilon(t-\tau)} K_{\alpha,\beta} d\tau \\ &= \mathcal{L}_{\alpha,\beta}(\mathfrak{X}(t_0))e^{-\epsilon(t-t_0)} + K_{\alpha,\beta}(1 - e^{-\epsilon(t-t_0)}).\end{aligned}$$

Thus, if $\mathcal{L}_{\alpha,\beta}(\mathfrak{X}(t)) \geq K_{\alpha,\beta},\ t \geq t_0$, the following inequality results

$$\mathcal{L}_{\alpha,\beta}(\mathfrak{X}(t)) - K_{\alpha,\beta} \leq [\mathcal{L}_{\alpha,\beta}(\mathfrak{X}(t_0)) - K_{\alpha,\beta}]e^{-\epsilon(t-t_0)}.$$

By calculating the limit, one has

$$\overline{\lim_{t\to\infty}}\mathcal{L}_{\alpha,\beta}(\mathfrak{X}(t)) \leq K_{\alpha,\beta}.$$

Therefore, the ellipsoid

$$\Psi_{\alpha,\beta}(\mathfrak{X}(t)) = \left\{\mathfrak{X} | \alpha x_1^2 + \beta x_2^2 + \beta x_4^2 + \beta(x_3 - \frac{\sigma\alpha + r\beta}{\beta})^2 + \beta(x_5 - \frac{\sigma\alpha + r\beta}{2\beta})^2 \leq K_{\alpha,\beta}\right\}$$

is the GEAS and PIS of system (2.8). This ends the proof. □

Different cases can be highlighted:
Case 1: For $\alpha = 1, \beta = 1$, then

$$\Psi_{1,1} = \left\{\mathfrak{X} | x_1^2 + x_2^2 + (x_3 - (\sigma + r))^2 + x_4^2 + (x_5 - \frac{\sigma + r}{2})^2 \leq \frac{11b}{7\epsilon}(\sigma + r)^2\right\},$$

is the GEAS of (2.8). Fore $\sigma = 10, b = \frac{8}{3}, r = 25$ and $d = \frac{19}{3}$, it yields

$$\Psi_{1,1} = \left\{\mathfrak{X} | x_1^2 + x_2^2 + (x_3 - 35)^2 + x_4^2 + (x_5 - \frac{35}{2})^2 \leq 71.6^2\right\}.$$

Figure 7 illustrates the attractors of (2.8) in distinct spaces by $\Psi_{1,1}$.

For $\sigma = 10, b = \frac{8}{3}, r = 43$ and $d = \frac{19}{3}$, results

$$\Psi_{1,1} = \left\{\mathfrak{X} | x_1^2 + x_2^2 + (x_3 - 53)^2 + x_4^2 + (x_5 - \frac{53}{2})^2 \leq 108.4^2\right\}.$$

Figure 8 shows the attractors in different spaces defined by $\Psi_{1,1}$.

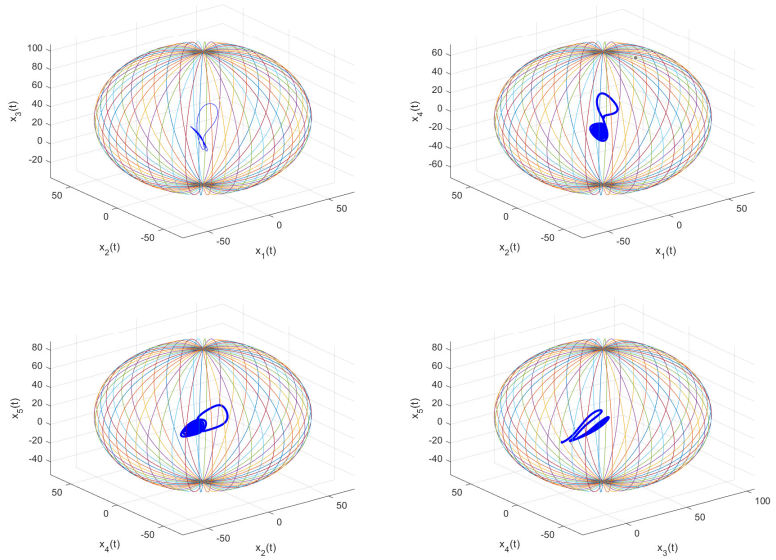

Figure 7. Phase portraits and GEAS of (2.8) with $\sigma = 10, b = \frac{8}{3}, r = 25$ and $d = \frac{19}{3}$.

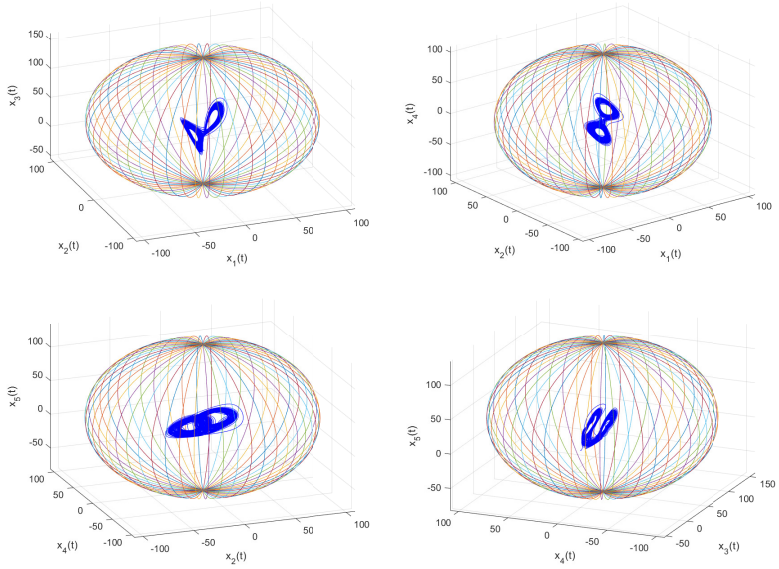

Figure 8. Phase portraits and GEAS of (2.8) with $\sigma = 10, b = \frac{8}{3}, r = 43$ and $d = \frac{19}{3}$.

Case 2: Let us consider $\alpha = 1, \beta = 2$. Thus, the set

$$\Psi_{1,2} = \left\{ \mathfrak{x} | x_1^2 + 2x_2^2 + 2(x_3 - \frac{a+2r}{2})^2 + 2x_4^2 + 2(x_5 - \frac{\sigma+2r}{4})^2 \leq \frac{11b}{14\epsilon}(\sigma+2r)^2 \right\},$$

is the GEAS of (2.8).

For $\sigma = 10, b = \frac{8}{3}, r = 25$ and $d = \frac{19}{3}$, we have

$$\Psi_{1,2} = \left\{ (x_1, x_2, x_3, x_4, x_5) | x_1^2 + 2x_2^2 + 2(x_3 - 30)^2 + 2x_4^2 + 2(x_5 - 15)^2 \leq 86.8^2 \right\}.$$

Case 3: Define $\alpha = 2, \beta = 1$. Then,

$$\Psi_{2,1} = \left\{ \mathfrak{X} | 2x_1^2 + x_2^2 + (x_3 - (2\sigma + r))^2 + x_4^2 + (x_5 - \frac{2\sigma + r}{2})^2 \leq \frac{11b}{7\epsilon}(2\sigma + r)^2 \right\},$$

is the GEAS of (2.8).

For $\sigma = 10, b = \frac{8}{3}, r = 25$ and $d = \frac{19}{3}$, one has

$$\Psi_{2,1} = \left\{ \mathfrak{X} | 2x_1^2 + x_2^2 + (x_3 - 45)^2 + x_4^2 + (x_5 - 22.5)^2 \leq 92.1^2 \right\}.$$

4. Accurate ultimate bound

In this section we derive a more accurate and smaller boundary set than that established by Theorem 3.1. We state the following theorem.

Theorem 4.1. *If $\sigma > 0, b > 0, r > 0$ and $d > 0$, then we have the following boundaries for system (2.8) variables:*

$$|x_1| \leq 2\sqrt{\frac{11b}{7}}\sqrt{\sigma r}, \tag{4.1}$$

$$|x_2| \leq \sqrt{\frac{11b}{7}}\, r, \tag{4.2}$$

$$|x_3 - \frac{\eta}{\sqrt{\beta}}| \leq \sqrt{\frac{11b}{7}}\, r, \tag{4.3}$$

$$|x_4| \leq \sqrt{\frac{11b}{7}}\, r, \tag{4.4}$$

$$|x_5 - \frac{\eta}{2\sqrt{\beta}}| \leq \sqrt{\frac{11b}{7}}\, r, \tag{4.5}$$

where

$$\eta = \frac{\sigma\alpha + r\beta}{\sqrt{\beta}}.$$

Proof. According to the results obtained from Theorem 3.1, we have

$$|x_1| \leq \sqrt{\frac{11b}{7}}\frac{\eta}{\sqrt{\alpha}},$$
$$|x_2| \leq \sqrt{\frac{11b}{7}}\frac{\eta}{\sqrt{\beta}},$$
$$|x_3 - \frac{\eta}{\sqrt{\beta}}| \leq \sqrt{\frac{11b}{7}}\frac{\eta}{\sqrt{\beta}},$$

$$|x_4| \leq \sqrt{\frac{11b}{7}}\frac{\eta}{\sqrt{\beta}},$$
$$|x_5 - \frac{\eta}{2\sqrt{\beta}}| \leq \sqrt{\frac{11b}{7}}\frac{\eta}{\sqrt{\beta}}.$$

It is clear from the above equations that the upper bound of $x_1, x_2, \ldots, x_5$, depends on the lower bound of $\frac{\eta}{\sqrt{\alpha}}$ and $\frac{\eta}{\sqrt{\beta}}$:

$$\frac{\eta}{\sqrt{\alpha}} = \frac{\sigma\sqrt{\alpha}}{\sqrt{\beta}} + \frac{r\sqrt{\beta}}{\sqrt{\alpha}} \geq 2\sqrt{\sigma r}.$$

Therefore, one can determine the bound for x_1 as shown in Eq (4.1). For variables x_2, x_3, x_4 and x_5, there is the same term:

$$\frac{\eta}{\sqrt{\beta}} = \frac{\sigma\alpha}{\beta} + r.$$

Let us take $\frac{\alpha}{\beta} = \frac{1}{N}$ with $N \in \mathbb{N}$. Therefore,

$$\sqrt{\frac{11b}{7}}\frac{\eta}{\sqrt{\beta}} = (\frac{1}{N}\sigma + r)\sqrt{\frac{11b}{7}}.$$

Since

$$\bigcap_{N=1}^{\infty}\{x_2 \in R||x_2| \leq (\frac{1}{N}\sigma + r)\sqrt{\frac{11b}{7}}\} = \{x_2 \in \mathbb{R}||x_2| \leq \sqrt{\frac{11b}{7}}r\},$$

we find a more limited boundary set for x_2 as shown in Eq (4.2), and by doing the same process one can obtain

$$\bigcap_{N=1}^{\infty}\{x_3 \in R||x_3 - \frac{\eta}{\sqrt{\beta}}| \leq (\frac{1}{N}\sigma + r)\sqrt{\frac{11b}{7}}\} = \{x_3 \in \mathbb{R}||x_3 - \frac{\eta}{\sqrt{\beta}}| \leq \sqrt{\frac{11b}{7}}r\},$$
$$\bigcap_{N=1}^{\infty}\{x_4 \in R||x_4| \leq (\frac{1}{N}\sigma + r)\sqrt{\frac{11b}{7}}\} = \{x_4 \in \mathbb{R}||x_4| \leq \sqrt{\frac{11b}{7}}r\},$$
$$\bigcap_{N=1}^{\infty}\{x_5 \in R||x_5 - \frac{\eta}{2\sqrt{\beta}}| \leq (\frac{1}{N}\sigma + r)\sqrt{\frac{11b}{7}}\} = \{x_5 \in \mathbb{R}||x_5 - \frac{\eta}{2\sqrt{\beta}}| \leq \sqrt{\frac{11b}{7}}r\}.$$

To confirm the theoretical results, we fix $\sigma = 10, b = \frac{8}{3}, r = 25$ and $d = \frac{19}{3}$. Figure 9, shows the estimated bounds for each state variable. Furthermore, Table 2 compares the bounds estimated by Theorems 3.1 and 4.1, showing the advantage of Theorem 4.1.

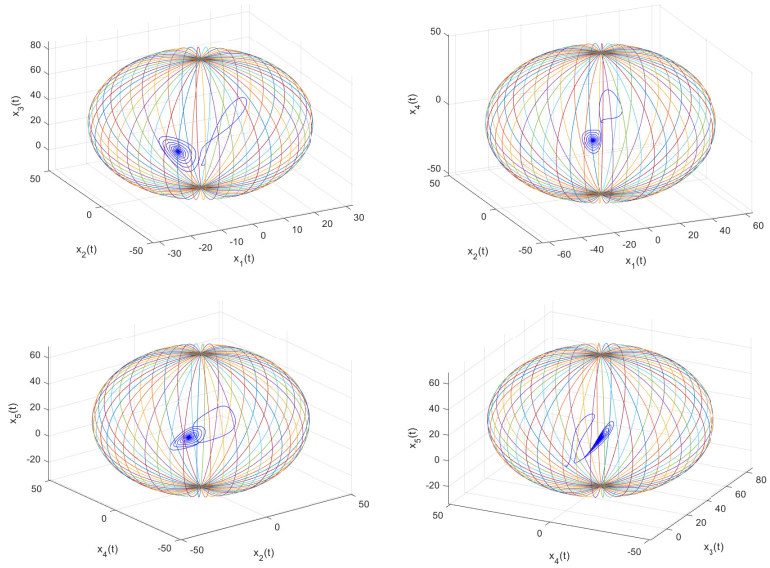

Figure 9. The phase portraits and GEAS of (2.8) with $\sigma = 10, b = \frac{8}{3}, r = 25$ and $d = \frac{19}{3}$.

Table 2. The bounds for system (2.8).

	Theorem 3.1	Theorem 4.1	Numerical results
x_1	(-71.6,71.6)	(-64.5,64.5)	(-18.3,19.7)
x_2	(-71.6,71.6)	(-51.1,51.1)	(-23.4,25.9)
x_3	(-36.6,106.6)	(-16.1,86.1)	(0.93,37.6)
x_4	(-71.6,71.6)	(-51.1,51.1)	(-7.73,8.98)
x_5	(-54.1,89.1)	(-33.6,68.6)	(0.06,19.6)

□

Remark 4.1. *A noteworthy point in calculating the bound for system (2.8) based on Theorem 4.1 is that the estimated boundary, in addition to being smaller, is independent of parameters β and α.*

5. Finite-time synchronization of the 5DLM

This section addresses the finite time synchronization of the 5DLM. In order to achieve fast and reliable synchronization, we use the results obtained in the previous section for the ultimate bound of (2.8). Let us consider the 5DLM (2.8) as the master, and define the slave by:

$$\begin{aligned} \dot{y}_1 &= \sigma(y_2 - y_1) + u_1, \\ \dot{y}_2 &= -y_1y_3 + ry_1 - y_2 + u_2, \\ \dot{y}_3 &= y_1y_2 - y_1y_4 - by_3 + u_3, \\ \dot{y}_4 &= y_1y_3 - 2y_1y_5 - dy_4 + u_4, \\ \dot{y}_5 &= 2y_1y_4 - 4by_5 + u_5, \end{aligned} \tag{5.1}$$

where y_1, y_2, y_3, y_4, y_5 are state vectors. The control law u_1, u_2, u_3, u_4, u_5 is designed for the drive (2.8) and response (5.1) systems can reach synchronization in finite time.

Lemma 5.1. *Suppose that $a_1, a_2, \cdots, a_n$ are real numbers and that $0 < s < 1$. Then, we have:*

$$(\sum_{i=1}^{n} a_i)^s \leq \sum_{i=1}^{n} a_i^s.$$

Lemma 5.2. *Inequality $2ab \leq \epsilon a^2 + \frac{1}{\epsilon} b^2$ holds for all real numbers $\epsilon > 0, a > 0$ and $b > 0$.*

Lemma 5.3. *Let us assume that $\mathcal{L}(t)$ is a continuous and positive-definite function that satisfies:*

$$\dot{\mathcal{L}}(t) \leq -\lambda \mathcal{L}(t) - \mu \mathcal{L}^{\omega}(t), \quad \forall t \geq 0, \quad \mathcal{L}(0) > 0. \tag{5.2}$$

Then, the system is exponentially finite-time stable, where $\lambda, \mu > 0$, and $0 < \omega < 1$ are constants.

Lemma 5.4. *Let us suppose that $\mathcal{L}(t)$ is a Lyapunov function satisfying Eq. (5.2). Then, it holds*

$$\mathcal{L}^{1-\omega}(t) \leq -(\frac{\mu}{\lambda}) + \frac{e^{ln[\lambda \mathcal{L}^{1-\omega}(0)+\mu] - \lambda(1-\omega)(t-0)}}{\lambda}, \quad 0 \leq t \leq T$$

and $\mathcal{L}(t) = 0, \quad \forall t \geq T$. The finite time T is

$$T^* = \frac{ln(\frac{\lambda \mathcal{L}^{1-\omega}(0)}{\mu} + 1)}{\lambda(1-\omega)}. \tag{5.3}$$

Definition 5.1. *Let us consider $\delta(t) = [\delta_1(t)\ \delta_2(t)\ \delta_3(t)\ \delta_4(t)\ \delta_5(t)]^T$, and define $\delta_i(t) = y_i(t) - x_i(t)$ as the synchronization errors. If there exists a positive value T^* such that*

$$\lim_{t \to T^*} \| \delta(t) \| = 0, \tag{5.4}$$

and $\| \delta(t) \| = 0$, for $t \geq T^*$, then the systems (2.8) and (5.1), achieve finite-time synchronization.

The next theorem states the exponential finite-time synchronization condition of systems (2.8) and (5.1).

Theorem 5.1. *The systems (2.8) and (5.1) can achieve finite-time synchronization by the control law:*

$$\begin{cases} u_1(t) = -\left(\lambda + 5\sqrt{\frac{22b}{7}} r + \sqrt{2}(\sigma + r)\right)\delta_1(t) - \mu \delta_1^s(t), \\ u_2(t) = -\left(\lambda + \frac{1}{2}\sqrt{\frac{11b}{14}} r\right)\delta_2(t) - \mu \delta_2^s(t), \\ u_3(t) = -\left(\lambda + \sqrt{\frac{11b}{14}} r\right)\delta_3(t) - \mu \delta_3^s(t), \\ u_4(t) = -\left(\lambda + \frac{5}{2}\sqrt{\frac{11b}{14}} r + \frac{(\sigma+r)}{\sqrt{2}}\right)\delta_4(t) - \mu \delta_4^s(t), \\ u_5(t) = -\left(\lambda + \sqrt{\frac{11b}{14}} r\right)\delta_5(t) - \mu \delta_5^s(t), \end{cases} \tag{5.5}$$

where $\lambda, \mu > 0$, *and* $s \in (0, 1)$. *Further, the systems are synchronized in the time*

$$T^* = \frac{ln(\frac{\lambda \mathcal{L}^{2(1-\omega)}(0)}{\mu} + 1)}{\lambda(1-\omega)}, \tag{5.6}$$

where $\omega = \frac{s+1}{2}$.

Proof. Theorem 4.1 provides an accurate estimate of the ultimate bound of variables of system (2.8). Let consider $\alpha = \beta = 1$, then $\eta = \sigma + r$. Therefore, we have

$$\begin{aligned} &|x_1| \leq 2\sqrt{\frac{11b}{7}}\sqrt{\sigma r},\ |x_2| \leq \sqrt{\frac{11b}{7}}r,\ |x_3 - (\sigma + r)| \leq \sqrt{\frac{11b}{7}}r, \\ &|x_4| \leq \sqrt{\frac{11b}{7}}r,\ |x_5 - \frac{\sigma + r}{2}| \leq \sqrt{\frac{11b}{7}}r. \end{aligned} \tag{5.7}$$

From (2.8) and (5.1), the following error dynamics results:

$$\begin{aligned} &\dot{\delta}_1 = \sigma(\delta_2 - \delta_1) + u_1, \\ &\dot{\delta}_2 = -y_1y_3 + ry_1 - y_2 + u_2 + x_1x_3 - rx_1 + x_2 \\ &= -(\delta_1 + x_1)(\delta_3 + x_3) + r(\delta_1 + x_1) - (\delta_2 + x_2) + u_2 + x_1x_3 - rx_1 + x_2 \\ &= -\delta_1\delta_3 - \delta_1x_3 - \delta_3x_1 + r\delta_1 - \delta_2 + u_2, \\ &\dot{\delta}_3 = y_1y_2 - y_1y_4 - by_3 + u_3 - x_1x_2 + x_1x_4 + bx_3 \\ &= (\delta_1 + x_1)(\delta_2 + x_2) - (\delta_1 + x_1)(\delta_4 + x_4) - b(\delta_3 + x_3) + u_3 - x_1x_2 + x_1x_4 + bx_3 \\ &= \delta_1\delta_2 + \delta_1x_2 + \delta_2x_1 - \delta_1\delta_4 - \delta_1x_4 - \delta_4x_1 - b\delta_3 + u_3, \\ &\dot{\delta}_4 = y_1y_3 - 2y_1y_5 - dy_4 + u_4 - x_1x_3 + 2x_1x_5 + dx_4 \\ &= (\delta_1 + x_1)(\delta_3 + x_3) - 2(\delta_1 + x_1)(\delta_5 + x_5) - d(\delta_4 + x_4) + u_4 - x_1x_3 + 2x_1x_5 + dx_4 \\ &= \delta_1\delta_3 + \delta_1x_3 + \delta_3x_1 - 2\delta_1\delta_5 - 2\delta_1x_5 - 2\delta_5x_1 - d\delta_4 + u_4, \\ &\dot{\delta}_5 = 2y_1y_4 - 4by_5 + u_5 - 2x_1x_4 + 4bx_5 \\ &= 2(\delta_1 + x_1)(\delta_4 + x_4) - 4b(\delta_5 + x_5) + u_5 - 2x_1x_4 + 4bx_5 \\ &= 2x_1\delta_4 + 2\delta_1x_4 + 2\delta_1\delta_4 - 4b\delta_5 + u_5. \end{aligned} \tag{5.8}$$

Let us consider the Lyapunov function:

$$\mathcal{L}_1(t) = \delta_1^2(t) + \delta_2^2(t) + \delta_3^2(t) + \delta_4^2(t) + \delta_5^2(t).$$

The time domain derivative of $\mathcal{L}(t)$ along the trajectories of (5.8) and using control law (5.5) is given by

$$\begin{aligned} &\frac{d\mathcal{L}_1(t)}{dt} = 2\delta_1\dot{\delta}_1 + 2\delta_2\dot{\delta}_2 + 2\delta_3\dot{\delta}_3 + 2\delta_4\dot{\delta}_4 + 2\delta_5\dot{\delta}_5 \\ &= 2\delta_1(\sigma\delta_2 - \sigma\delta_1 + u_1) + 2\delta_2(-\delta_1\delta_3 - \delta_1x_3 - \delta_3x_1 + r\delta_1 - \delta_2 + u_2) \\ &+2\delta_3(\delta_1\delta_2 + \delta_1x_2 + \delta_2x_1 - \delta_1\delta_4 - \delta_1x_4 - \delta_4x_1 - b\delta_3 + u_3) \\ &+2\delta_4(\delta_1\delta_3 + \delta_1x_3 + \delta_3x_1 - 2\delta_1\delta_5 - 2\delta_1x_5 - 2\delta_5x_1 - d\delta_4 + u_4) \\ &+2\delta_5(2x_1\delta_4 + 2\delta_1x_4 + 2\delta_1\delta_4 - 4b\delta_5 + u_5) \end{aligned}$$

$$
\begin{aligned}
&= -2\sigma\delta_1^2 - 2\delta_2^2 - 2b\delta_3^2 - 2d\delta_4^2 - 8b\delta_5^2 + 2(\sigma + r - x_3)\delta_1\delta_2 + 2\delta_1\delta_3 x_2 \\
&-2\delta_1\delta_3 x_4 + 2\delta_1\delta_4 x_3 - 4\delta_1\delta_4 x_5 + 4\delta_1\delta_5 x_4 \\
&+2\delta_1 u_1 + 2\delta_2 u_2 + 2\delta_3 u_3 + 2\delta_4 u_4 + 2\delta_5 u_5 \\
&\leq 2|\sigma + r - x_3||\delta_1||\delta_2| + 2|\delta_1||\delta_3||x_2| + 2|\delta_1||\delta_3||x_4| + 2|\delta_1||\delta_4||x_3| \\
&\quad + 4|\delta_1||\delta_4||x_5| + 4|\delta_1||\delta_5||x_4| + 2\delta_1 u_1 + 2\delta_2 u_2 + 2\delta_3 u_3 + 2\delta_4 u_4 + 2\delta_5 u_5 \\
&\leq 2\sqrt{\frac{11b}{7}}r|\delta_1||\delta_2| + 2\sqrt{\frac{11b}{7}}r|\delta_1||\delta_3| + 2\sqrt{\frac{11b}{7}}r|\delta_1||\delta_3| + 2(\sqrt{\frac{11b}{7}}r + \sigma + r)|\delta_1||\delta_4| \\
&+4(\sqrt{\frac{11b}{7}}r + \frac{\sigma + r}{2})|\delta_1||\delta_4| + 4\sqrt{\frac{11b}{7}}r|\delta_1||\delta_4| + 4\sqrt{\frac{11b}{7}}r|\delta_1||\delta_5|
\end{aligned}
$$

$$
\begin{aligned}
&+2\delta_1\left[-\left(\lambda + 5\sqrt{\frac{22b}{7}}r + \sqrt{2}(\sigma + r)\right)\delta_1(t) - \mu\delta_1^s(t)\right] \\
&+2\delta_2\left[-\left(\lambda + \frac{1}{2}\sqrt{\frac{11b}{14}}r\right)\delta_2(t) - \mu\delta_2^s(t)\right] + 2\delta_3\left[-\left(\lambda + \sqrt{\frac{11b}{14}}r\right)\delta_3(t) - \mu\delta_3^s(t)\right] \\
&+2\delta_4\left[-\left(\lambda + \frac{5}{2}\sqrt{\frac{11b}{14}}r + \frac{(\sigma + r)}{\sqrt{2}}\right)\delta_4(t) - \mu\delta_4^s(t)\right] \\
&+2\delta_5\left[-\left(\lambda + \sqrt{\frac{11b}{14}}r\right)\delta_5(t) - \mu\delta_5^s(t)\right].
\end{aligned}
$$

From Lemma 5.2, we have

$$
\begin{aligned}
2|\delta_1||\delta_2| &\leq \sqrt{2}\delta_1^2 + \frac{1}{\sqrt{2}}\delta_2^2, \\
2|\delta_1||\delta_3| &\leq \sqrt{2}\delta_1^2 + \frac{1}{\sqrt{2}}\delta_3^2, \\
2|\delta_1||\delta_4| &\leq \sqrt{2}\delta_1^2 + \frac{1}{\sqrt{2}}\delta_4^2, \\
2|\delta_1||\delta_5| &\leq \sqrt{2}\delta_1^2 + \frac{1}{\sqrt{2}}\delta_5^2.
\end{aligned} \tag{5.9}
$$

Then using Lemma 5.3, we obtain

$$
\begin{aligned}
\frac{d\mathcal{L}_1(t)}{dt} &\leq -2\lambda\delta_1^2 - 2\lambda\delta_2^2 - 2\lambda\delta_3^2 - 2\lambda\delta_4^2 - 2\lambda\delta_5^2 - 2\mu(\delta_1^{s+1} + \delta_2^{s+1} + \delta_3^{s+1} + \delta_4^{s+1} + \delta_5^{s+1}) \\
&\leq -2\lambda(\delta_1^2 + \delta_2^2 + \delta_3^2 + \delta_4^2 + \delta_5^2) - 2\mu(\delta_1^2 + \delta_2^2 + \delta_3^2 + \delta_4^2 + \delta_5^2)^{\frac{1+s}{2}} \\
&= -2\lambda\mathcal{L}(t) - 2\mu\mathcal{L}^{\omega}(t), \forall t \geq 0,
\end{aligned}
$$

where $\lambda, \mu > 0, \omega = \frac{1+s}{2}$. This implies that

$$
e^{2\lambda t}\frac{d\mathcal{L}_1(t)}{dt} + 2\lambda e^{2\lambda t}\mathcal{L}_1(t) = \frac{d}{dt}(e^{2\lambda t}\mathcal{L}_1(t)) \leq 0.
$$

Therefore,

$$\int_0^t \frac{d}{dt}(e^{2\lambda t}\mathcal{L}_1(t))dt = e^{2\lambda t}\mathcal{L}_1(t) - \mathcal{L}_1(0) \leq 0,$$

which leads to

$$\mathcal{L}_1(t) \leq e^{-2\lambda t}\mathcal{L}_1(0),$$

and since $\| \delta(t) \|^2 = \mathcal{L}_1(t)$, we obtain

$$\| \delta(t) \| \leq \sqrt{\mathcal{L}_1(0)}e^{-\lambda t}, \quad \forall t \geq 0.$$

This, from Lemma 5.3 and Lemma 5.4, guarantees the exponential synchronization of systems (2.8) and (5.1) in finite time T^*.

To be more realistic, an approach is presented here that requires only one controller to implement synchronization. □

Corollary 5.1. *When the control functions are chosen as*

$$\begin{aligned}
u_1 = &-\left(\lambda + 5\sqrt{\frac{22b}{7}}r + \sqrt{2}(\sigma + r)\right)\delta_1 - \left(\lambda + \frac{1}{2}\sqrt{\frac{11b}{14}}r\right)\frac{\delta_2^2}{\delta_1} \\
&-\left(\lambda + \sqrt{\frac{11b}{14}}r\right)\frac{\delta_3^2}{\delta_1} - \left(\lambda + \frac{5}{2}\sqrt{\frac{11b}{14}}r + \frac{(\sigma + r)}{\sqrt{2}}\right)\frac{\delta_4^2}{\delta_1} \\
&-\left(\lambda + \sqrt{\frac{11b}{14}}r\right)\frac{\delta_5^2}{\delta_1} - \mu\delta_1^s - \mu\frac{\delta_2^{s+1}}{\delta_1} - \mu\frac{\delta_3^{s+1}}{\delta_1} - \mu\frac{\delta_4^{s+1}}{\delta_1} - \mu\frac{\delta_5^{s+1}}{\delta_1}, \\
u_2 = u_3 = u_4 = u_5 = 0,
\end{aligned} \tag{5.10}$$

then, the drive system (2.8) is exponentially synchronized with the slave system (5.1).

Proof. The Lyapunov function is selected as

$$\mathcal{L}(t) = \delta_1^2(t) + \delta_2^2(t) + \delta_3^2(t) + \delta_4^2(t) + \delta_5^2(t).$$

In view of (5.8) and (5.10), the derivative of $\mathcal{L}(t)$ is

$$\begin{aligned}
\frac{d\mathcal{L}_1(t)}{dt} &= -2\sigma\delta_1^2 - 2\delta_2^2 - 2b\delta_3^2 - 2d\delta_4^2 - 8b\delta_5^2 + 2(\sigma + r - x_3)\delta_1\delta_2 + 2\delta_1\delta_3 x_2 \\
&\quad -2\delta_1\delta_3 x_4 + 2\delta_1\delta_4 x_3 - 4\delta_1\delta_4 x_5 + 4\delta_1\delta_5 x_4 + 2\delta_1 u_1 \\
&\leq 2|\sigma + r - x_3||\delta_1||\delta_2| + 2|\delta_1||\delta_3||x_2| + 2|\delta_1||\delta_3||x_4| + 2|\delta_1||\delta_4||x_3| \\
&\quad + 4|\delta_1||\delta_4||x_5| + 4|\delta_1||\delta_5||x_4| + 2\delta_1 u_1 \\
&\leq 2\sqrt{\frac{11b}{7}}r|\delta_1||\delta_2| + 2\sqrt{\frac{11b}{7}}r|\delta_1||\delta_3| + 2\sqrt{\frac{11b}{7}}r|\delta_1||\delta_3| \\
&\quad +2(\sqrt{\frac{11b}{7}}r + \sigma + r)|\delta_1||\delta_4| + 4(\sqrt{\frac{11b}{7}}r + \frac{\sigma + r}{2})|\delta_1||\delta_4|
\end{aligned}$$

$$+4\sqrt{\frac{11b}{7}}r|\delta_1||\delta_4| + 4\sqrt{\frac{11b}{7}}r|\delta_1||\delta_5| - 2\left(\lambda + 5\sqrt{\frac{22b}{7}}r + \sqrt{2}(\sigma + r)\right)\delta_1^2$$

$$-2\left(\lambda + \frac{1}{2}\sqrt{\frac{11b}{14}}r\right)\delta_2^2 \quad -2\left(\lambda + \sqrt{\frac{11b}{14}}r\right)\delta_3^2 - 2\left(\lambda + \frac{5}{2}\sqrt{\frac{11b}{14}}r + \frac{(\sigma + r)}{\sqrt{2}}\right)\delta_4^2$$

$$-2\left(\lambda + \sqrt{\frac{11b}{14}}r\right)\delta_5^2 - 2\mu\delta_1^s - 2\mu\delta_2^{s+1} - 2\mu\delta_3^{s+1} - 2\mu\delta_4^{s+1} - 2\mu\delta_5^{s+1}.$$

According to Lemma 5.2, Lemma 5.3 and (5.9) we have

$$\begin{aligned}\frac{d\mathcal{L}_1(t)}{dt} &\leq -2\lambda\delta_1^2 - 2\lambda\delta_2^2 - 2\lambda\delta_3^2 - 2\lambda\delta_4^2 - 2\lambda\delta_5^2 - 2\mu(\delta_1^{s+1} + \delta_2^{s+1} + \delta_3^{s+1} + \delta_4^{s+1} + \delta_5^{s+1}) \\ &\leq -2\lambda(\delta_1^2 + \delta_2^2 + \delta_3^2 + \delta_4^2 + \delta_5^2) - 2\mu(\delta_1^2 + \delta_2^2 + \delta_3^2 + \delta_4^2 + \delta_5^2)^{\frac{1+s}{2}} \\ &= -2\lambda\mathcal{L}(t) - 2\mu\mathcal{L}^{\omega}(t), \forall t \geq 0,\end{aligned}$$

where $\lambda, \mu > 0, \omega = \frac{1+s}{2}$. Therefore, synchronization is achieved exponentially with the control law (5.10).

To show the effectiveness of the control proposed in theorem 5.1, we perform numerical simulations. Let us choose the initial conditions $x_1(0) = 1$, $x_2(0) = -1$, $x_3(0) = 2$, $x_4(0) = 1$, $x_5(0) = 1$, $y_1(0) = 0.1$, $y_2(0) = 0.1$, $y_3(0) = 0.2$, $y_4(0) = -1$, $y_5(0) = 1$, and other parameters as $\lambda = 1$, $\mu = 1$ and $s = \frac{1}{3}$. Figure 10 depicts the time series of the drive system (2.8) and the response system (5.1) without input control, in which the goal of synchronization has not been achieved. Figure 11 shows the case of using the proposed control (5.5). We verify that system (5.1) exponentially synchronizes with the master system (2.8) within the guaranteed convergence time.

The synchronization error for different modes with different controllers are depicted in Figure 12. The noteworthy point in these figures is that the goal of synchronization is achieved faster by increasing the number of controllers.

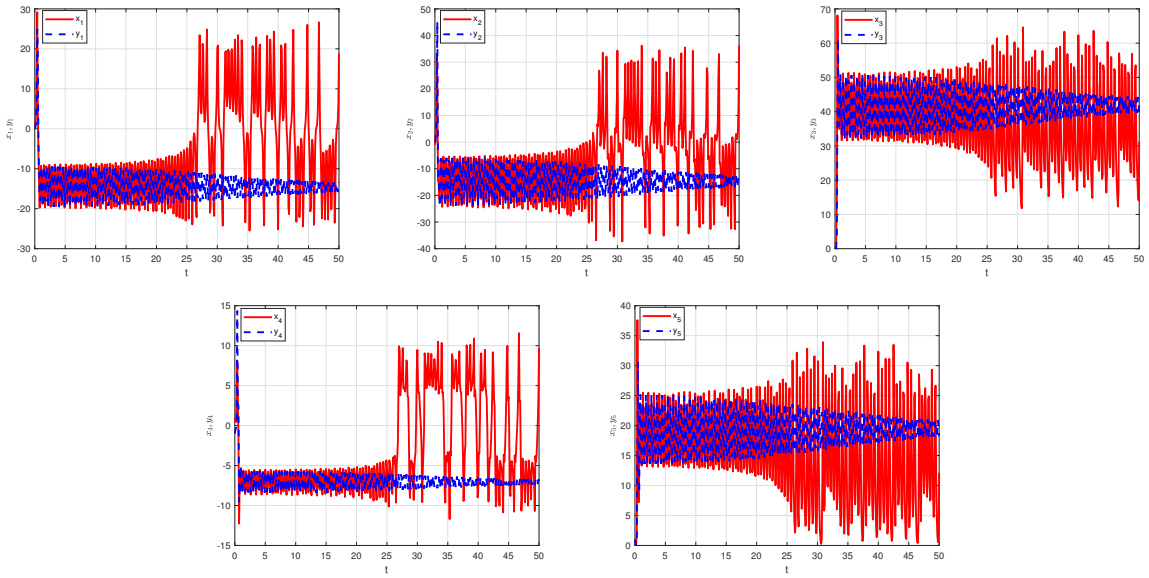

Figure 10. State trajectories of the drive and response systems without control input.

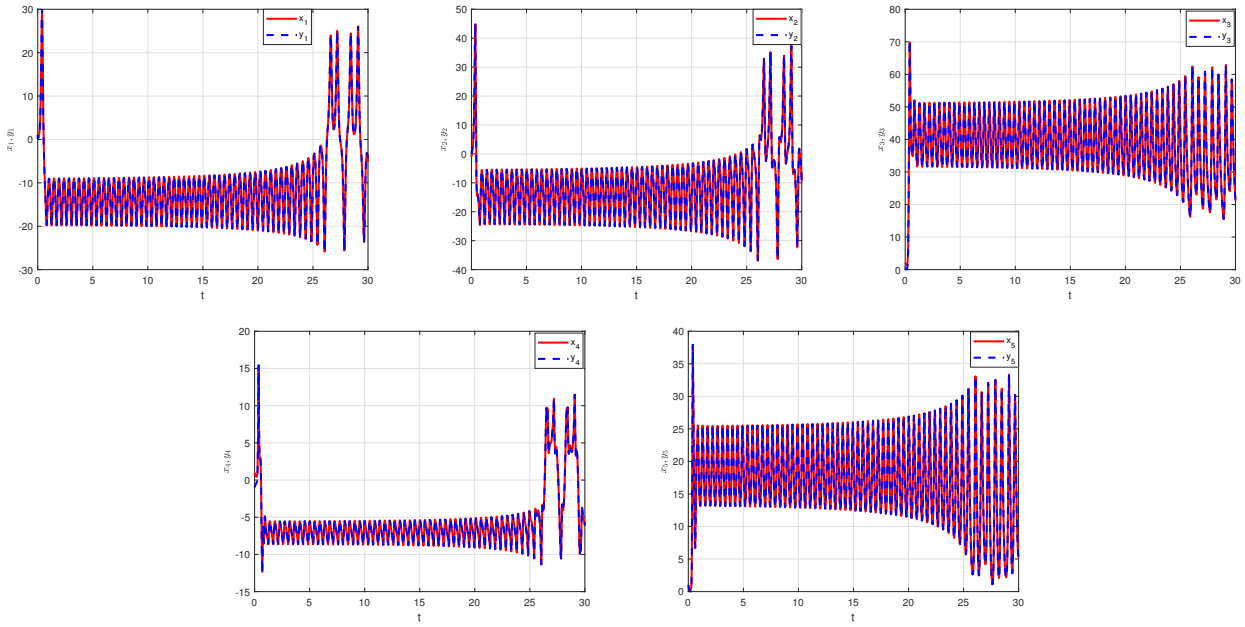

Figure 11. State trajectories of the drive and response systems with one control input.

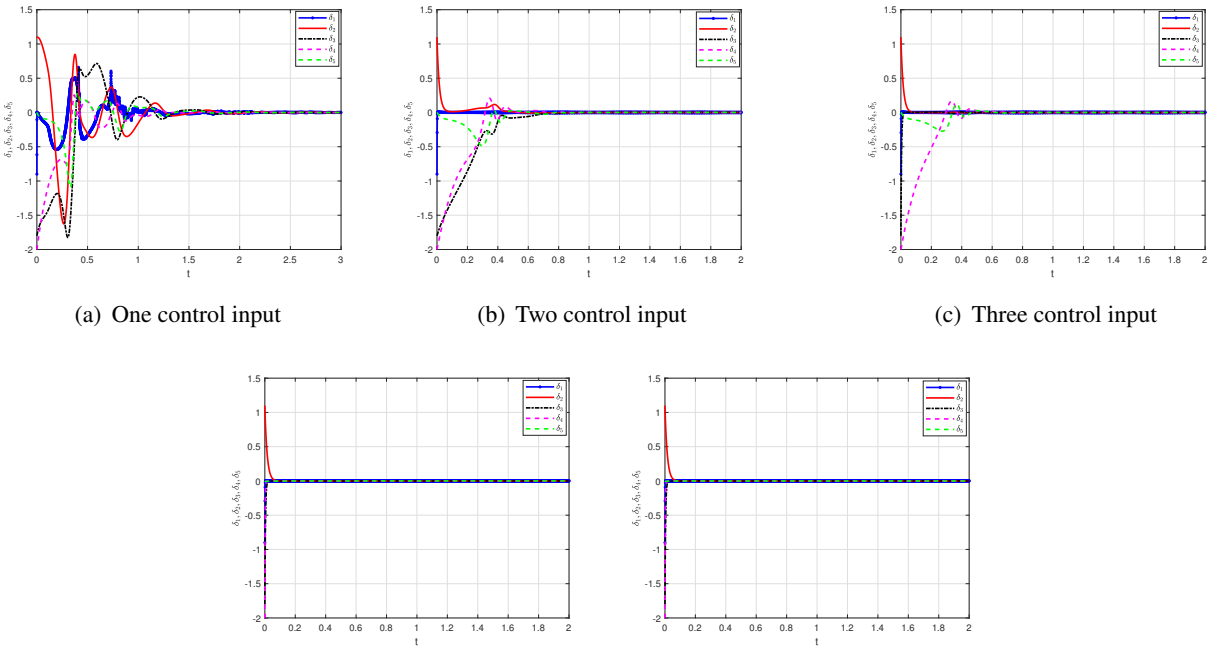

(a) One control input (b) Two control input (c) Three control input

(d) Four control input (e) Five control input

Figure 12. Synchronization errors with different control inputs.

□

6. Conclusions

The global dynamics of the 5DLM, which was obtained by increasing two modes to the original Lorenz system, was analyzed. Phase portraits, bifurcation diagrams and GEAS were estimated. Due to the dependence of the GEAS on the free parameters, a new boundary for the variables was estimated, which is more accurate than the existing one. Also, by employing a finite time control scheme, a synchronization method was proposed based on the obtained ultimate bound sets. The corresponding boundedness was numerically verified to demonstrate the efficiency of the presented method.

Use of AI tools declaration

The authors declare they have not used Artificial Intelligence (AI) tools in the creation of this article.

Conflict of interest

The authors declare that there are no conflicts of interests regarding the publication of this article.

References

1. G. Chen, T. Ueta, Yet another chaotic attractor, *Int. J. Bifurcat. Chaos*, **9** (1999), 1465–1466. https://doi.org/10.1142/S0218127499001024
2. S. Celikovsky, G. Chen, On a generalized Lorenz canonical form of chaotic systems, *Int. J. Bifurcat. Chaos*, **12** (2002), 1789–1812. https://doi.org/10.1142/S0218127402005467
3. E. N. Lorenz, Deterministic nonperiodic flow, *J. Atmos. Sci.*, **20** (1963), 130–141.
4. B. Saltzman, Finite amplitude free convection as an initial value problem, *J. Atmos. Sci.*, **19** (1962), 329–341.
5. E. Lorenz, The predictability of hydrodynamic flow, *Trans. N. Y. Acad. Sci.*, **25** (1963), 409–432.
6. X. Hu, B. Sang, N. Wang, The chaotic mechanisms in some jerk systems, *AIMS Math.*, **7** (2022), 15714–15740. http://dx.doi.org/10.3934/math.2022861
7. F. Zhang, K. Sun, Y. Chen, H. Zhang, C. Jiang, Parameters identification and adaptive tracking control of uncertain complex-variable chaotic systems with complex parameters, *Nonlinear Dyn.*, **95** (2019), 3161–3176. https://doi.org/10.1007/s11071-018-04747-z
8. S. Celikovsky, G. Chen, On the generalized Lorenz canonical form, *Chaos Solit. Fract.*, **26** (2005), 1271–1276. https://doi.org/10.1016/j.chaos.2005.02.040
9. S. Celikovsky, G. Chen, Generalized Lorenz canonical form revisited, *Int. J. Bifurcat. Chaos*, **31** (2021), 2150079. https://doi.org/10.1142/S0218127421500796
10. F. Zhang, S. Zhang, G. Chen, C. Li, Z. Li, C. Pan, Special attractors and dynamic transport of the hybrid-order complex Lorenz system, *Chaos Solit. Fract.*, **164** (2022), 112700. https://doi.org/10.1016/j.chaos.2022.112700
11. S. H. Salih, N. M. G. Al-Saidi, 3D-Chaotic discrete system of vector borne diseases using environment factor with deep analysis, *AIMS Math.*, **7** (2022), 3972–3987. http://doi.org/10.3934/math.2022219

12. A. Bushra Abdulshakoor M, W. Liu, Li-Yorke chaotic property of cookie-cutter systems, *AIMS Math.*, **7** (2022), 13192–13207. https://doi.org/10.3934/math.2022727

13. L. Chen, H. Yin, L. Yuan, A. M. Lopes, J. T. Machado, R. Wu, A novel color image encryption algorithm based on a fractional-order discrete chaotic neural network and DNA sequence operations, *Front. Inform. Technol. Electron. Eng.*, **21** (2020), 866–879. https://doi.org/10.1631/FITEE.1900709

14. L. Chen, W. Pan, R. Wu, J. T. Machado, A. M. Lopes, Design and implementation of grid multi-scroll fractional-order chaotic attractors, *Chaos*, **26** (2016), 084303. https://doi.org/10.1063/1.4958717

15. J. Li, N. Cui, A hyperchaos generated from Rabinovich system, *AIMS Math.*, **8** (2023), 1410–1426. http://doi.org/10.3934/math.2023071

16. B. W. Shen, Nonlinear feedback in a five-dimensional Lorenz model, *J. Atmos. Sci.*, **71** (2014), 1701–1723. https://doi.org/10.1175/JAS-D-13-0223.1

17. S. Faghih-Naini, B. W. Shen, Quasi-periodic orbits in the five-dimensional non-dissipative Lorenz model: the role of the extended nonlinear feedback loop, *Int. J. Bifurcat. Chaos*, **28** (2018), 1850072. https://doi.org/10.1142/S0218127418500724

18. B. W. Shen, Nonlinear feedback in a six-dimensional Lorenz model: impact of an additional heating term, *Nonlin. Processes Geophys.*, **22** (2015), 749–764. https://doi.org/10.5194/npg-22-749-2015

19. B. W. Shen, Hierarchical scale dependence associated with the extension of the nonlinear feedback loop in a seven-dimensional Lorenz model, *Nonlin. Processes Geophys.*, **23** (2016), 189–203. https://doi.org/10.5194/npg-23-189-2016

20. B. W. Shen, Aggregated negative feedback in a generalized Lorenz model, *Int. J. Bifurcat. Chaos*, **29** (2019), 1950037. https://doi.org/10.1142/S0218127419500378

21. G. Leonov, A. Bunin, N. Koksch, Attractor localization of the Lorenz system, *ZAMM*, **67** (1987), 649–656.

22. G. Leonov, N. Kuznetsov, Hidden attractors in dynamical systems. From hidden oscillations in Hilbert–Kolmogorov, Aizerman, and Kalman problems to hidden chaotic attractor in Chua circuits, *Int. J. Bifurc. Chaos Appl. Sci. Eng.*, **23** (2013), 1330002. https://doi.org/10.1142/S0218127413300024

23. C. Feng, L. Li, Y. Liu, Z. Wei, Global dynamics of the chaotic disk dynamo system driven by noise, *Complexity*, **2020** (2020), 8375324. https://doi.org/10.1155/2020/8375324

24. Y. Li, Z. Wei, A. A. Aly, A 4D hyperchaotic Lorenz-type system: zero-Hopf bifurcation, ultimate bound estimation, and its variable-order fractional network, *Eur. Phys. J. Spec. Top.*, **231** (2022), 1847–1858. https://doi.org/10.1140/epjs/s11734-022-00448-2

25. J. Jian, Z. Zhao, New estimations for ultimate boundary and synchronization control for a disk dynamo system, *Nonlinear Anal. Hybrid Syst.*, **9** (2013), 56–66. https://doi.org/10.1016/j.nahs.2012.12.002

26. H. Saberi Nik, S. Effati, J. Saberi-Nadjafi, New ultimate bound sets and exponential finite-time synchronization for the complex Lorenz system, *J. Complexity*, **31** (2015), 715–730. https://doi.org/10.1016/j.jco.2015.03.001
27. P. C. Rech , Hyperchaos and quasiperiodicity from a four-dimensional system based on the Lorenz system, *Eur. Phys. J. B.*, **90** (2017), 251. https://doi.org/10.1140/epjb/e2017-80533-5
28. W. Gao, L. Yan, M-H. Saeedi, H. Saberi Nik, Ultimate bound estimation set and chaos synchronization for a financial risk system, *Math. Comput. Simulat.*, **154** (2018), 19–33. https://doi.org/10.1016/j.matcom.2018.06.006
29. X. Zhang, Dynamics of a class of non-autonomous Lorenz-type systems, *Int. J. Bifurcat. Chaos*, **26** (2016), 1650208. https://doi.org/10.1142/S0218127416502084
30. P. Swinnerton-Dyer, Bounds for trajectories of the Lorenz equations:an illustration of how to choose Liapunov functions, *Phys. Lett A*, **281** (2001), 161–167. https://doi.org/10.1016/S0375-9601(01)00109-8
31. F. Chien, A. R. Chowdhury, H. Saberi Nik, Competitive modes and estimation of ultimate bound sets for a chaotic dynamical financial system, *Nonlinear Dynam.*, **106** (2021), 3601–3614. https://doi.org/10.1007/s11071-021-06945-8
32. F. Chien, M. Inc, H-R.Yosefzade, H. Saberi Nik, Predicting the chaos and solution bounds in a complex dynamical system, *Chaos Solitons Fract.*, **153** (2021), 111474. https://doi.org/10.1016/j.chaos.2021.111474
33. H. Wang , X. Li , A note on "Hopf bifurcation analysis and ultimate bound estimation of a new 4-D quadratic autonomous hyper-chaotic system" in [Appl. Math. Comput. 291 (2016) 323–339] by Amin Zarei and Saeed Tavakoli, *Appl. Math. Comput.*, **329** (2018), 1–4. https://doi.org/10.1016/j.amc.2018.01.027
34. H. Wang, G. Dong, New dynamics coined in a 4-D quadratic autonomous hyper-chaotic system, *Appl. Math. Comput.*, **346** (2019), 272–286. https://doi.org/10.1016/j.amc.2018.10.006
35. Y. Xie, P. Zhou, J. Ma, Energy balance and synchronization via inductive-coupling in functional neural circuits, *Appl. Math. Model.*, **113** (2023), 175–187. https://doi.org/10.1016/j.apm.2022.09.015
36. A. G. Radwan, K. Moaddy, K. N. Salama, S. Momani, I. Hashim, Control and switching synchronization of fractional order chaotic systems using active control technique, *J. Adv. Res.*, **5** (2014), 125–132. https://doi.org/10.1016/j.jare.2013.01.003
37. N. Cui, J. Li, A new 4D hyperchaotic system and its control, *AIMS Math.*, **8** (2023), 905–923. http://dx.doi.org/10.3934/math.2023044
38. Y. He, J. Peng, S. Zheng, Fractional-order financial system and fixed-time synchronization, *Fractal Fract.*, **6** (2022), 507. https://doi.org/10.3390/fractalfract6090507
39. I. Ahmad, A. Ouannas, M. Shafiq, V. T. Pham, D. Baleanu, Finite-time stabilization of a perturbed chaotic finance model, *J. Adv. Res.*, **32** (2021), 1–14. https://doi.org/10.1016/j.jare.2021.06.013
40. D. Vivek, K. Kanagarajan, E. M. Elsayed, Some existence and stability results for Hilfer-fractional implicit differential equations with nonlocal conditions, *Mediterr. J. Math.*, **15**, (2018), 15. https://doi.org/10.1007/s00009-017-1061-0

41. X. Leng, B. Du, S. Gu, S. He, Novel dynamical behaviors in fractional-order conservative hyperchaotic system and DSP implementation, *Nonlinear Dynam.*, **109** (2022), 1167–1186. https://doi.org/10.1007/s11071-022-07498-0

42. A. M. A. El-Sayed, H. M. Nour, A. Elsaid, A. E. Matouk, A. Elsonbaty, Dynamical behaviors, circuit realization, chaos control, and synchronization of a new fractional order hyperchaotic system, *Appl. Math. Model.*, **40** (2016), 3516–3534. https://doi.org/10.1016/j.apm.2015.10.010

43. P. Zhou, X. K. Hu, Z. G. Zhu, J. Ma, What is the most suitable Lyapunov function? *Chaos Solit. Fract.*, **150** (2021), 111154. https://doi.org/10.1016/j.chaos.2021.111154

AIMS Press